REGULAR ARTICLE

blood advances

Phf6-null hematopoietic stem cells have enhanced self-renewal capacity and oncogenic potentials

Yueh-Chwen Hsu,[1] Tsung-Chih Chen,[2,3] Chien-Chin Lin,[1,3] Chang-Tsu Yuan,[4] Chia-Lang Hsu,[5] Hsin-An Hou,[2] Chein-Jun Kao,[1] Po-Han Chuang,[1] Yu-Ren Chen,[1] Wen-Chien Chou,[1,2] and Hwei-Fang Tien[2]

[1]Department of Laboratory Medicine and [2]Division of Hematology, Department of Internal Medicine, National Taiwan University Hospital, Taipei, Taiwan; [3]Graduate Institute of Clinical Medicine, College of Medicine, National Taiwan University, Taipei, Taiwan; and [4]Department of Pathology and [5]Department of Medical Research, National Taiwan University Hospital, Taipei, Taiwan

Key Points

- Phf6 deletion enhances HSC reconstitution and self-renewal and lowers the threshold of *NOTCH1*-induced T-cell acute lymphoblastic leukemia.
- Aged Phf6 knockout mice develop myelodysplasia-like diseases.

Plant homeodomain finger gene 6 (*PHF6*) encodes a 365-amino-acid protein containing 2 plant homology domain fingers. Germline mutations of human *PHF6* cause Börjeson-Forssman-Lehmann syndrome, a congenital neurodevelopmental disorder. Loss-of-function mutations of *PHF6* are detected in patients with acute leukemia, mainly of T-cell lineage and in a small proportion of myeloid lineage. The functions of PHF6 in physiological hematopoiesis and leukemogenesis remain incompletely defined. To address this question, we generated a conditional *Phf6* knockout mouse model and investigated the impact of *Phf6* loss on the hematopoietic system. We found that *Phf6* knockout mice at 8 weeks of age had reduced numbers of $CD4^+$ and $CD8^+$ T cells in the peripheral blood compared with the wild-type littermates. There were decreased granulocyte-monocytic progenitors but increased $Lin^-c\text{-}Kit^+Sca\text{-}1^+$ cells in the marrow of young *Phf6* knockout mice. Functional studies, including competitive repopulation unit and serial transplantation assays, revealed an enhanced reconstitution and self-renewal capacity in *Phf6* knockout hematopoietic stem cells (HSCs). Aged *Phf6* knockout mice had myelodysplasia-like presentations, including decreased platelet counts, megakaryocyte dysplasia, and enlarged spleen related to extramedullary hematopoiesis. Moreover, we found that *Phf6* loss lowered the threshold of *NOTCH1*-induced leukemic transformation at least partially through increased leukemia-initiating cells. Transcriptome analysis on the restrictive rare HSC subpopulations revealed upregulated cell cycling and oncogenic functions, with alteration of key gene expression in those pathways. In summary, our studies show the in vivo crucial roles of Phf6 in physiological and malignant hematopoiesis.

Introduction

Plant homeodomain finger gene 6 (*PHF6*) encodes a protein of 365 amino acids with 2 plant homology domain fingers.[1] The PHF6 protein is highly conserved in vertebrate species.[2] Expression of *Phf6* is high in embryonic and early fetal phases; in adult tissues, *Phf6* expression is low except for the projection neurons. It is supposed to regulate chromatin structure. In some cell lines, PHF6 physically interacts with nucleosome remodeling and deacetylation complex.[3] Knockdown of *PHF6* impairs proliferation and arrests cell cycle progression in HeLa cells.[4] PHF6 is also involved in transcriptional control, which orchestrates neuron migration in the brain.[5] However, the detailed functions of PHF6 have not yet been well defined.

Submitted 3 May 2019; accepted 21 June 2019. DOI 10.1182/bloodadvances.2019000391.

The full-text version of this article contains a data supplement.

The next-generation sequencing data reported in this article have been deposited in the Gene Expression Omnibus database (accession number GSE129465).

Mutations in *PHF6* were first described in patients with Börjeson-Forssman-Lehmann syndrome, a congenital neurodevelopmental anomaly.[6] Subsequently, mutations of this gene were identified in T-cell acute lymphoblastic leukemia (T-ALL).[7] Loss-of-function mutations, including deletions, nonsense, missense, or frameshift mutations of *PHF6*, were reported in 16% of pediatric patients[8] and 38% of adult T-ALL patients and 3% of patients with acute myeloid leukemia (AML).[9] Thus, *PHF6* seems to be a tumor suppressor gene in both settings. Interestingly, knockout of *Phf6* impaired the proliferation of precursor B acute lymphoblastic leukemia cells in vivo.[10,11] Hence, it is likely that *PHF6* has context- and lineage-dependent effects in leukemogenesis.

To examine the roles of *Phf6* mutations in leukemogenesis, recent reports of *Phf6* knockout mouse models indicated that absence of *Phf6* enhanced hematopoietic stem cell (HSC) self-renewal capacity[12,13] and lowered the threshold of the development of oncogenic *NOTCH1*-induced T-ALL.[12] Loss of *Phf6* resulted in hematopoietic neoplasms after a relatively long period, and *TLX3* overexpression enhanced leukemic transformation.[14]

The current report describes another *Phf6*-knockout mouse model. We found that the mutant mice had reduced numbers of $CD4^+$ and $CD8^+$ T cells in their peripheral blood compared with the wild-type littermates. Under steady state, young *Phf6* knockout mice had enriched $Lin^-c\text{-}Kit^+Sca\text{-}1^+$ (LSK) cells in the marrow, but the number of long-term HSCs (LT-HSCs) did not differ. Functional studies, including serial transplantation and competitive repopulation unit (CRU) assays, revealed an enhanced self-renewal and competitive reconstitution capacity of *Phf6*-deficient HSCs. Aged *Phf6* knockout mice developed myelodysplasia-like disease, including decreased platelet counts, megakaryocyte dysplasia, and enlarged spleen related to extramedullary hematopoiesis. In addition, we found that *Phf6* loss lowered the threshold of *NOTCH1*-induced leukemic transformation at least partially through increased leukemia-initiating cells (LICs). Transcriptome sequencing, Gene Ontology, and Gene Set Enrichment Analysis (GSEA) of LT-HSCs and type 2 and type 3 multipotent progenitors (MPP2 and MPP3) showed enriched cell cycle and oncogenic functions in *Phf6* knockout HSCs. Several key genes in these pathways were significantly altered in *Phf6*-null cells. Our results, together with recently published reports, revealed the crucial functions of *PHF6* in physiological and malignant hematopoiesis.

Methods

Generation of *Phf6* conditional knockout mice

Using the CRISPR/Cas9 technique, exon 2 to exon 11 of *Phf6* were flanked by 2 LoxP sequences. The mice were mated with *vavCre* transgenic mice expressing the Cre recombinase under control of the *vav* promoter to knock out *Phf6* in the hematopoietic cells at the embryonic stage.[15] Because *Phf6* is at the X chromosome, we mated *Phf6* hemizygous male mice carrying heterozygous *vavCre* transgene ($Phf6^{F/Y}$;$vavCre^{Tg/+}$) with homozygous female mice without the *vavCre* transgene ($Phf6^{F/F}$;$vavCre^{+/+}$). Expectedly, one half of their offspring were *Phf6* wild-type ($Phf6^{F/Y}$;$vavCre^{+/+}$ and $Phf6^{F/F}$;$vavCre^{+/+}$), and the other half were *Phf6* knockout ($Phf6^{F/Y}$;$vavCre^{Tg/+}$ and $Phf6^{F/F}$;$vavCre^{Tg/+}$) mice. Animals were housed in the clean conventional animal facility, and all procedures were approved by the Institutional Animal Care and Use Committee of National Taiwan University College of Medicine.

Bone marrow transplantation and CRU assay

Bone marrow cells (BMCs) harvested from wild-type or *Phf6* knockout mice were used for bone marrow transplantation. B6.SJL-$Ptprc^{\alpha}pepc^{\beta}$/BoyJ (CD45.1) recipient mice were lethally irradiated with a single dose of 10 Gy. Then 10^6 unfractionated donor BMCs (CD45.2) were administered to each recipient by retro-orbital injection within 24 hours. The chimerism of $CD45.2^+$ cells in the peripheral blood of recipient mice was evaluated every 4 weeks. Bone marrow was examined 16 weeks after transplantation. For secondary transplantations, we transplanted sorted $CD45.2^+$ wild-type or $CD45.2^+$ *Phf6* knockout cells from the first recipient into each lethally irradiated recipient. Peripheral blood and bone marrow were inspected at the same schedule as the primary recipients.

In the CRU assay, 2×10^5 of $CD45.1^+$ whole BMCs were used as helper cells; $CD45.2^+$ *Phf6* knockout or wild-type BMCs were the test cells. Test cells were mixed with $CD45.1^+$ helper cells and transplanted into lethally irradiated $CD45.1^+$ recipient mice. Peripheral blood was analyzed for the proportion of $CD45.1^+$ and $CD45.2^+$ cells every 4 weeks.

Retroviral transduction of *NOTCH1*

Wild-type and *Phf6* knockout donor mice were injected with 150 mg/kg of 5-fluorouracil (Merck, Darmstadt, Germany) 4 days before harvesting bone marrow. Retrovirus construct carrying intracellular *NOTCH1* (*ICN1*) was transfected into a Plat-E retroviral packaging cell line (Cell Biolabs, San Diego, CA) 3 days before viral transduction. To the day of viral transduction, bone marrow of donor mice was harvested, and the conditioned medium was filtered through a 0.22-μm syringe filter and concentrated via Amicon Ultra-15 Centrifugal Filter Units (Merck). The virus concentrate was then applied to the mouse bone marrow cultured in StemSpan SFEM II (Stemcell Technologies, Vancouver, BC, Canada) complete medium with protamine sulfate 5 μg/mL, recombinant mouse stem cell factor 50 ng/mL, recombinant mouse interleukin-3 10 ng/mL, recombinant mouse Flt3 ligand 50 ng/mL, and recombinant human thrombopoietin 50 ng/mL. After 72 hours, vital cells with green fluorescence (GFP^+) were sorted and transplanted into lethally irradiated recipients for further experiments.

Limiting dilution analysis of LICs

Leukemic cells were sorted from the bone marrow of recipient mice harboring wild-type cells with *ICN1* overexpression (WT+*ICN1*) or *Phf6* null cells with *ICN1* overexpression (*Phf6* KO+*ICN1*) according to GFP expression. Lethally irradiated recipients received 300 000 helper cells plus either 100 000, 30 000, 10 000, or 3000 sorted GFP^+ BMCs. Four to 5 weeks after transplantation, peripheral blood of the recipient mice was sampled to evaluate the chimerism. The mice were monitored for 6 months. An extreme limiting dilution analysis tool was used to calculate the LIC numbers.[16]

Fluorescence-activated cell sorting analysis and cell sorting

We analyzed the populations of LT-HSCs ($Lin^-Sca\text{-}1^+c\text{-}Kit^+CD150^+CD48^-$), MPP2 ($Lin^-Sca\text{-}1^+c\text{-}Kit^+CD150^+CD48^+$), MPP3 ($Lin^-Sca\text{-}1^+c\text{-}Kit^+CD150^-CD48^+$), common myeloid progenitors (CMP) ($Lin^-Sca\text{-}1^-c\text{-}Kit^+CD34^+Fc\gamma R^{lo}$), granulocyte-monocytic progenitors (GMP) ($Lin^-Sca\text{-}1^-c\text{-}Kit^+CD34^+Fc\gamma R^{hi}$),

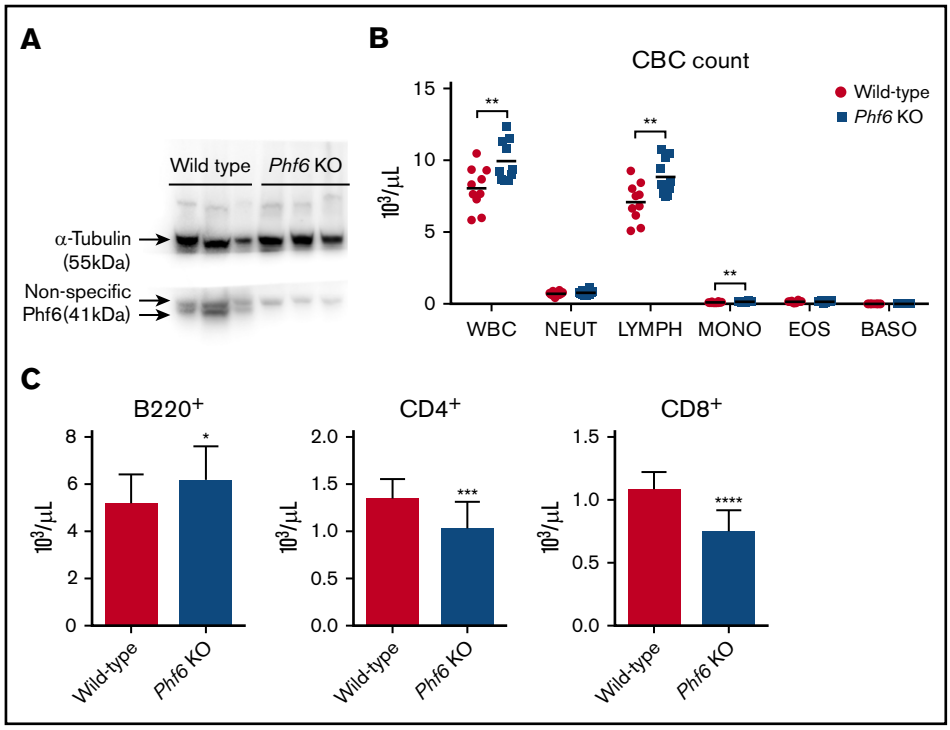

Figure 1. Cell counts in the peripheral blood of mice 8 to 12 weeks of age. (A) Western hybridization of BMCs harvested from 3 wild-type mice (left 3 lanes) and 3 *Phf6* knockout (KO) mice (right 3 lanes). Phf6 (~41 kDa) was markedly depleted in the bone marrow of *Phf6* KO mice. (B) Female *Phf6* KO mice had higher WBC, lymphocyte (LYMPH), and monocyte (MONO) counts than wild-type littermates. (C) *Phf6* KO mice (n = 19), male and female, had higher $B220^+$ B-cell counts (left panel), lower $CD4^+$ T-cell counts (middle panel), and lower $CD8^+$ T-cell counts (right panel) in their peripheral blood than wild-type mice (n = 17). $^*P < .05$; $^{**}P < .01$; $^{***}P < .001$; $^{****}P < .0001$. BASO, basophil; CBC, complete cell count; EOS, eosinophil; NEUT, neutrophil.

megakaryocyte-erythroid progenitors ($Lin^-Sca\text{-}1^-c\text{-}Kit^+CD34^-Fc\gamma R^{lo}$), and LICs ($CD4^-CD8^-CD25^+CD127^+$).[17] Splenocytes were grouped into B cells ($B220^+TCR\beta^-$) and T cells ($B220^-TCR\beta^+$). T cells included CD4 single-positive cells ($B220^-TCR\beta^+CD4^+CD8^-$) and CD8 single-positive cells ($B220^-TCR\beta^+CD4^-CD8^+$). Within the fraction of CD4 single-positive cells, we analyzed naive regulatory T cells ($B220^-TCR\beta^+CD4^+CD8^-CD25^+$) and effector T cells ($B220^-TCR\beta^+CD4^+CD8^-CD25^-$). B cells included total B cells ($CD19^+B220^+$), pro-B cells ($B220^+CD19^+IgD^-IgM^-CD2^-$), pre–B cells ($B220^+CD19^+IgD^-IgM^-CD2^+$), immature B cells ($B220^+CD19^+IgD^-IgM^+CD2^+$), and mature B cells ($B220^+CD19^+IgD^+IgM^+CD2^+$).[18] For cell cycle analysis, anti–Ki-67 was used to label cells in G0 phase ($Ki\text{-}67^-$) and G1/S/G2/M phase ($Ki\text{-}67^+$); propidium iodide was used to detect cells in G1, S, or G2/M phases. Flow cytometry analysis was performed on BD LSRII, BD LSRFortessa, or BD FACSVerse flow cytometers (BD Biosciences, Franklin Lakes, NJ). Target cells were sorted by using a BD FACSAriaIII multicolor cell sorter (BD Biosciences). Data were analyzed by using FlowJo software (FlowJo, Ashland, OR).

Next-generation sequencing of HSCs

We sorted 100 to 200 cells of LT-HSCs, MPP2, and MPP3 from the mice, followed by RNA extraction and complementary DNA synthesis according to a SMART-Seq V4 ultra Low Input RNA kit (Clontech Laboratories, Mountain View, CA) and a SMART-Seq HT kit (Clontech). Libraries were prepared by using a Nextera XT DNA sample preparation kit (Illumina, San Diego, CA). Transcriptome sequencing was performed on the NextSeq 500 platform (Illumina).

Analysis of the gene expression profile

Raw reads were aligned to mouse reference genome GRCm38 and expression then quantified by using STAR software.[19] Read counts were normalized by the trimmed mean of the M-values method implemented in the R package edgeR.[20] For preranked GSEA, differential expression analysis was performed between cells from *Phf6* knockout and wild-type mice using limma,[21] and a ranking metric was calculated for each gene as $r = -\log_{10}(p) * \text{sign}(\log_2 \text{fold-change})$, where p is the significance of differentially expression analysis. Preranked GSEA implemented in the R package clusterProfiler[22] was performed by using the Gene Ontology and oncogenic gene sets from the Molecular Signature Database. For Gene Ontology gene sets, those significantly enriched ($P < .05$) in at least 2 cell types were visualized as an Enrichment Map[23] with a cutoff >0.2 Jaccard-overlap combination score.

Statistical analysis

Data were processed in Microsoft Excel (Microsoft, Redmond, WA) or GraphPad Prism (GraphPad Software, La Jolla, CA) software. Student *t* test or paired Student *t* tests were used to compare the differences between groups.

Results

Peripheral blood analyses in the *Phf6* knockout and wild-type mice

The deletion of Phf6 in hematopoietic cells was confirmed by immunoblotting (Figure 1A). At 8 weeks, female *Phf6* knockout mice (n = 10) had higher counts of white blood cells (WBC) ($P = .0094$), monocytes ($P = .0076$), and lymphocytes ($P = .0074$) compared with female wild-type mice (n = 10) (Figure 1B). These differences were not seen in male mice, however (supplemental Figure 1). We found that *Phf6* knockout mice (n = 19) had higher counts of $B220^+$ B cells ($P = .0329$) but lower counts of $CD4^+$ ($P = .0009$) and $CD8^+$ ($P < .0001$) T cells in the peripheral blood compared with wild-type mice (n = 17) according to fluorescence-activated cell sorting (FACS) analysis (Figure 1C).

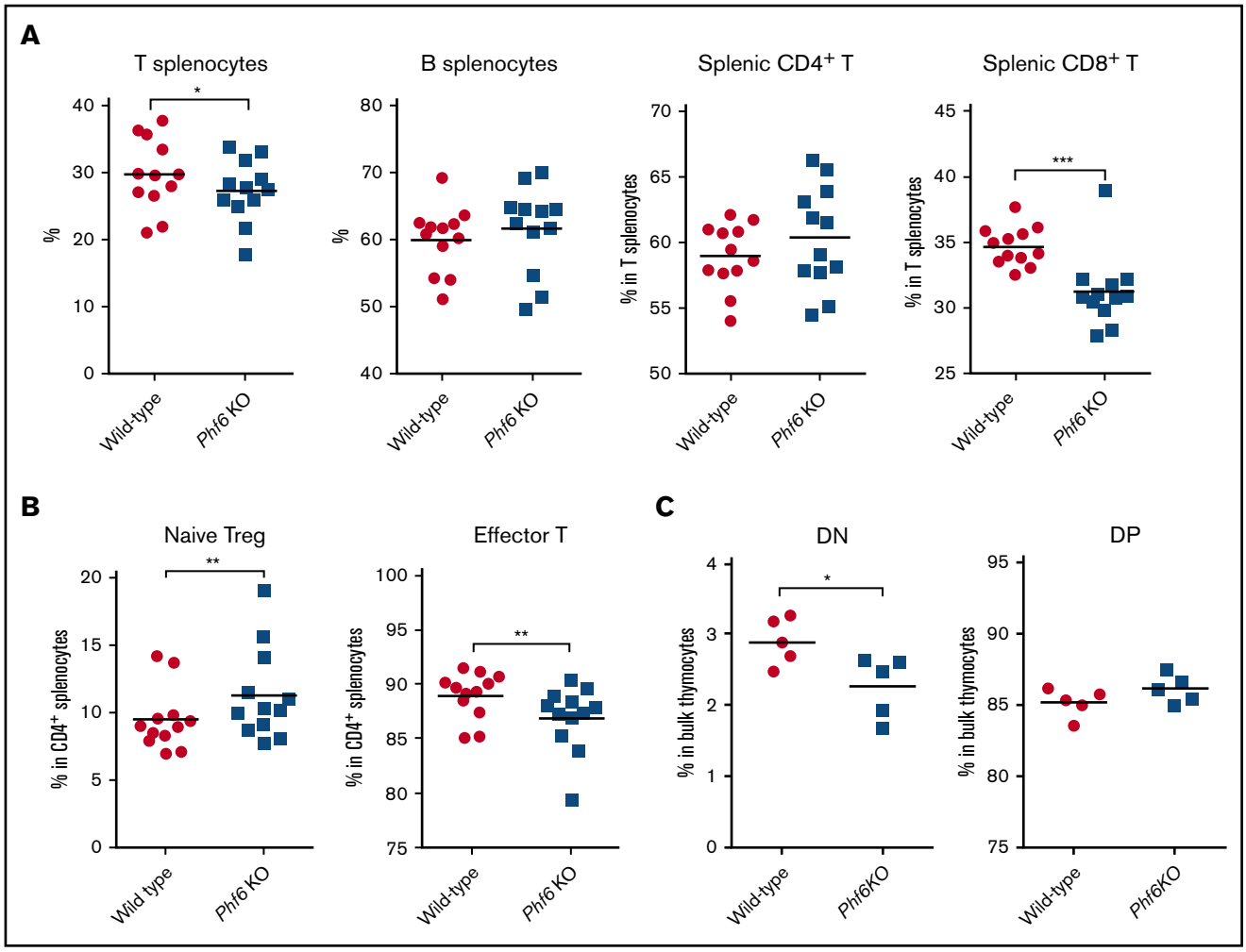

Figure 2. Lymphocyte composition in the spleen and thymus of mice 8 to 12 weeks of age. (A) The percentages of T cells ($P = .0372$), especially $CD8^+$ T cells ($P = .001$), in the spleen were lower in *Phf6* knockout (KO) mice than in *Phf6* wild-type mice (wild-type, n = 12; *Phf6* KO, n = 12), whereas the B-cell and $CD4^+$ T-cell percentages did not differ. (B) Within $CD4^+$ splenocytes, *Phf6* KO mice had higher percentages of naive regulatory T cells (Treg) (left panel; $P = .0076$) but lower percentages of effector T cells (right panel; $P = .0043$; wild-type, n = 12; *Phf6* KO, n = 12). (C) Within thymocytes, *Phf6* KO mice had lower percentages of CD4 and CD8 double-negative (DN) cells compared with wild-type mice ($P = .0316$; both, n = 5). $^*P < .05$; $^{**}P < .01$; $^{***}P < .001$. DP, CD4 and CD8 double-positive cells.

Analyses of splenocytes and thymocytes in the *Phf6* knockout and wild-type mice

The weights of spleen and thymus of *Phf6* knockout mice were not different from wild-type mice at 8 to 12 weeks of age (supplemental Figure 2). The histology sections also look similar between the 2 groups of mice. However, in the spleen, *Phf6* knockout mice (n = 12) had a lower percentage of T cells ($P = .0372$) compared with the wild-type mice (n = 12), but the percentage of B cells was not different (Figure 2A). *Phf6* knockout mice had a lower percentage of $CD8^+$ T cells ($P = .001$) but not $CD4^+$ T cells compared with the wild-type mice. Within the $CD4^+$ T-cell compartment, the *Phf6* knockout mice had a higher percentage of naive regulatory T cells ($B220^-TCR\beta^+CD4^+CD8^-CD25^+$) ($P = .0076$) (Figure 2B) and a lower percentage of effector T cells ($B220^-TCR\beta^+CD4^+CD8^-CD25^-$) ($P = .0043$). However, we could not detect any differences in the functions of the total T cells (supplemental Figure 3), naive regulatory T cells, or effector T cells (data not shown) between the 2 groups of mice through cytokine stimulation assays (supplemental Methods). The CD4 and CD8 double-negative thymocytes in *Phf6* knockout mice were decreased compared with the wild-type littermates ($P = .0316$) (Figure 2C); other populations of thymocytes remained similar between the 2 groups of mice (supplemental Figure 4).

Bone marrow analyses in the *Phf6* knockout and wild-type mice

Phf6 depletion did not affect the architecture and cellularity of bone marrow at 8 to 12 weeks of age (supplemental Figure 5). However, there were increased pro-B cells (n = 6; $P = .0429$), but the other B-cell subpopulations were similar to the wild-type mice (Figure 3A). The mutant mice had reduced GMPs (n = 6; $P = .0184$) (Figure 3B). *Phf6* depletion decreased Lin^- cells (n = 6; $P = .0008$) (supplemental Figure 6) and $Lin^-Sca\text{-}1^+c\text{-}Kit^-$ (LK) cells (n = 6, $P = .011$); conversely, LSK cells (n = 11; $P = .0187$) (Figure 3C) and MPP2s (n = 11; $P = .0035$) (Figure 3D) were increased in marrow. The percentage of LT-HSCs was not altered by *Phf6* deletion. A lower proportion of MPP3 cells from *Phf6* knockout mice

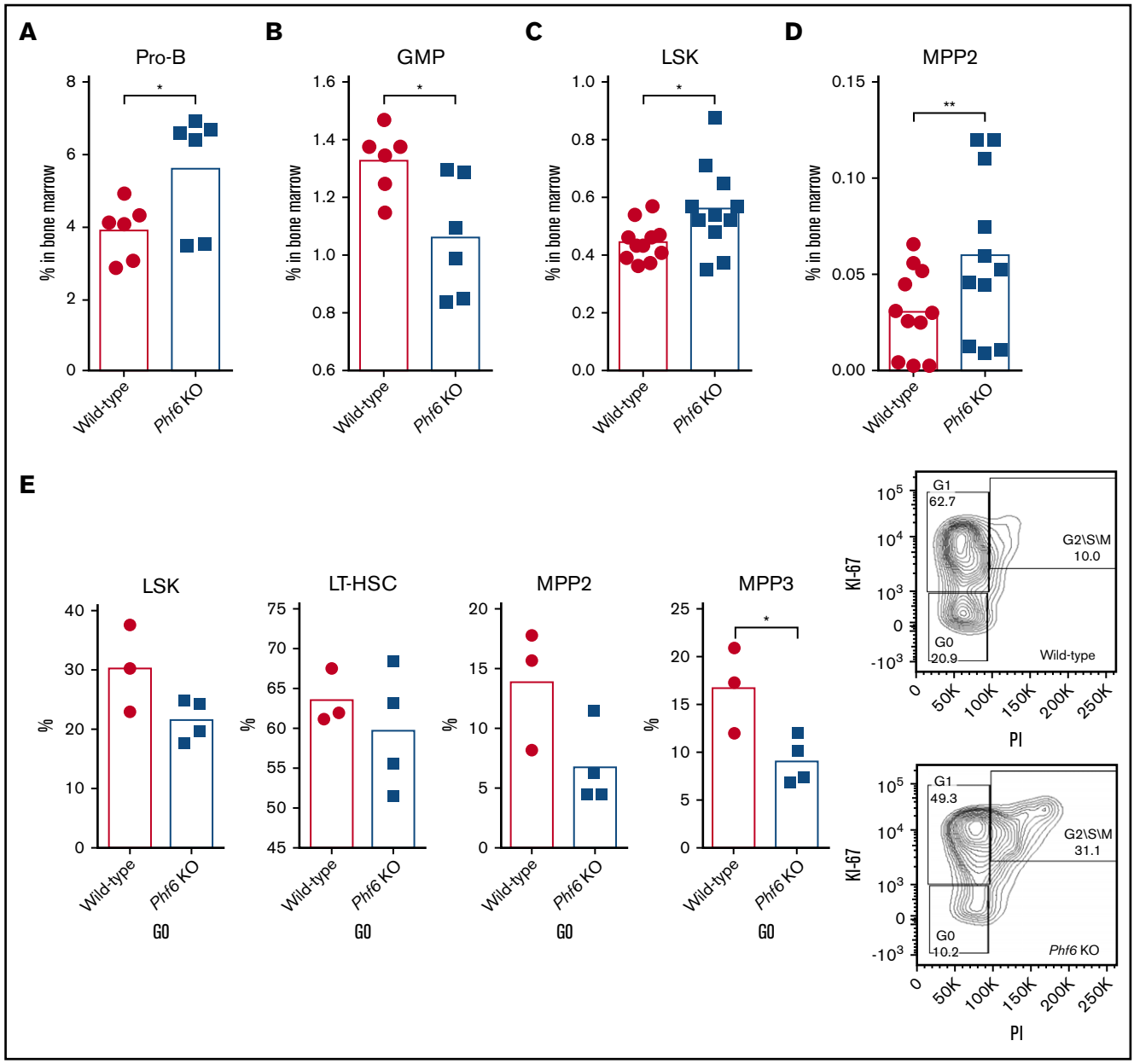

Figure 3. The composition of HSPCs under steady state. (A) *Phf6* knockout (KO) mice had higher percentages of pro-B cells in their bone marrow ($P = .0429$; wild-type, n = 6; *Phf6* KO, n = 6). (B) *Phf6* KO mice had less GMP ($P = .0184$; wild-type, n = 11; *Phf6* KO, n = 11). (C) *Phf6* KO mice had higher percentages of LSK BMCs compared with wild-type mice ($P = .0187$; wild-type, n = 11; *Phf6* KO, n = 11). (D) The percentages of MPP2 were higher in *Phf6* KO mice ($P = .0035$; wild-type, n = 11; *Phf6* KO, n = 11). (E) Cell cycle analysis of the subpopulations of *Phf6* KO HSPCs exhibited a lower proportion of G0 phase cells compared with the wild-type counterparts. Representative FACS plots showed more active proliferation in *Phf6* KO MPP3 compared with the wild-type cells.*$P < .05$; **$P < .01$.

(n = 4) were in G0 phase than wild-type littermates (n = 3; $P = .0323$) (Figure 3E). Similar trends were also seen in MPP2, LT-HSC, and bulk LSK cells. These results suggest a more active cell division and proliferation in the *Phf6* knockout hematopoietic stem/progenitor cells (HSPCs).

HSPC analyses in the aged *Phf6* knockout mice and wild-type littermates

There were no evident changes in hemogram in *Phf6*-null mice until 18 months of age when *Phf6* knockout mice (n = 21) had lower lymphocyte ($P = .0237$) and platelet ($P = .0002$) counts in the blood compared with wild-type mice (n = 20) (Figure 4A-B). Counts of $B220^+$ B cells ($P = .0345$), $CD4^+$ T cells ($P = .0126$), and $CD8^+$ T cells ($P = .0258$) were lower in aged *Phf6* knockout mice compared with aged wild-type littermates (Figure 4C-E). Spleens of the aged *Phf6* knockout mice (n = 10) were significantly larger ($P = .014$) than the wild-type littermates (n = 7) (Figure 4F). Histology examination revealed enhanced extramedullary hematopoiesis in the red pulp of spleens from *Phf6* knockout mice (Figure 4G). Bone marrow cellularity was similar between the 2 groups of mice, but megakaryocytes of *Phf6* knockout mice were

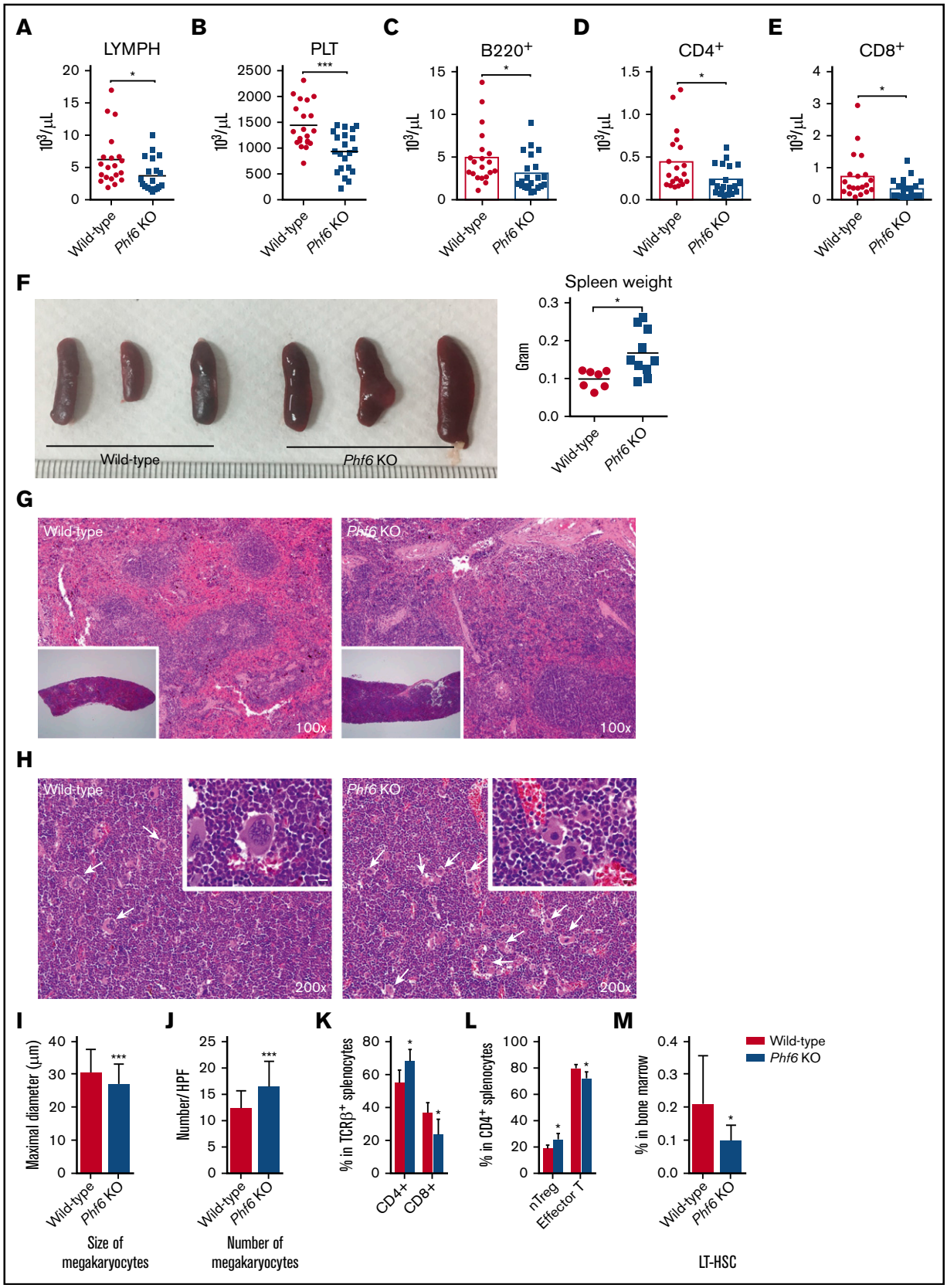

Figure 4. Analysis of aged wild-type and *Phf6* knockout (KO) mice. (A) At 18 months of age, *Phf6* KO mice had lower lymphocyte (LYMPH) counts ($P = .0237$; wild-type, n = 20; *Phf6* KO, n = 21). (B) Aged wild-type mice had higher platelet (PLT) counts compared with aged *Phf6* KO mice ($P = .0002$; wild-type, n = 20; *Phf6* KO,

hyperplastic and dysplastic, and had hypolobulated nuclei (Figure 4H; supplemental Figure 7), smaller size ($P = .0007$) (both n = 3) (Figure 4I), and higher number ($P = .0004$) (Figure 4J). Within the spleens, there was a higher percentage of $CD4^+$ cells ($P = .0105$) and a lower percentage of $CD8^+$ cells ($P = .0247$) in the *Phf6* knockout mice (Figure 4K) (wild-type, n = 5; *Phf6* knockout, n = 9). Similar to the young mice, the aged *Phf6* knockout mice (n = 9) had a higher percentage of naive regulatory T cells ($P = .018$) and a lower percentage of effector T cells ($P = .0205$) compared with wild-type mice (n = 5) (Figure 4L). Different from the young mice, the aged *Phf6* knockout mice (n = 10) had reduced LT-HSCs ($P = .0424$) compared with wild-type mice (n = 7) (Figure 4M).

Analyses of reconstitution capability of hematopoietic cells from the *Phf6* knockout and wild-type mice

CRU assays were used to test the reconstitution capacity of hematopoiesis of *Phf6* knockout mice. We found significantly higher chimerism ($P = .0312$) in recipients transplanted with *Phf6* knockout bulk BMCs (n = 7) compared with those transplanted with wild-type bulk BMCs (n = 7) (Figure 5A). *Phf6* knockout graft yielded higher percentages of Lin^- cells ($P = .0065$), $Lin^-Sca\text{-}1^-c\text{-}Kit^+$ (LK) cells ($P = .000169$), GMP ($P = .0037$), and megakaryocyte-erythroid progenitors ($P = .0032$) (Figure 5B). The functional advantage of *Phf6* knockout cells was validated by higher chimerism in recipients transplanted with sorted LSK cells ($P = .0478$) (wild-type, n = 9; *Phf6* knockout, n = 8). These results suggested that HSCs of *Phf6* knockout mice had higher reconstitution capability compared with those of wild-type mice.

Analyses of self-renewal capability of HSCs from the *Phf6* knockout and wild-type mice

To further test the self-renewal capacity of HSCs from the *Phf6* knockout mice, we transplanted bulk BMCs from mice 8 to 12 weeks of age without helper cells into lethally irradiated recipient mice. Peripheral blood was analyzed every month after transplantation. Nine months after transplantation, recipient mice transplanted with *Phf6* knockout BMCs (n = 9) had higher counts of WBC ($P = .0239$) (Figure 5C) and granulocytes ($P < .0001$) but lower counts of lymphocytes ($P = .0036$) compared with the recipients transplanted with wild-type BMCs (n = 8). We also observed higher percentages of donor-derived $CD11b^+Gr1^-$ cells ($P = .0022$) but lower percentages of $CD4^+$ ($P = .0262$) and $CD8^+$ ($P = .0041$) cells in the blood of recipients transplanted with *Phf6*-deficient BMCs (Figure 5D). By secondary transplantation, we found that the *Phf6*-deficient donor cells yielded even higher chimerism in both the peripheral blood ($P = .0005$) (Figure 5E) and marrow ($P = .001$) of their recipients (n = 7) compared with wild-type BMCs (n = 6). Similar results were seen when the donor cells were harvested from aged mice (18 months old) (supplemental Figure 8). These results suggested that *Phf6*-deficient mice exhibited stronger reconstitution capability and self-renewal capacity.

The effects of *Phf6* deletion in the development of *NOTCH1*-induced leukemia

Our data showed that *Phf6* deletion was insufficient for leukemogenesis after an 18-month observation period, although there were myelodysplasia-like phenotypes, including thrombocytopenia (Figure 4B), megakaryocyte dysplasia (Figure 4H), and extramedullary hematopoiesis in spleens (Figure 4G). Our goal was to determine if *Phf6* deletion functioned as an oncogenic adjunct in leukemogenesis of lymphoid cell lineage. *NOTCH1* is the most commonly mutated gene in human T-ALL.[24] Overexpression of *ICN1* could induce T-ALL in mice.[25] We transplanted either WT+*ICN1* or *Phf6* KO+*ICN1* cells into recipient mice 8 to 12 weeks of age. We found that *Phf6* KO+*ICN1* mice had more aggressive phenotypes than WT+*ICN1* mice, including lower hemoglobin levels ($P = .0353$) (Figure 6A), and a trend of higher counts of WBC and neutrophils, lower platelet counts, and higher lactate dehydrogenase levels (supplemental Figure 9A). The leukemic marrow of both WT+*ICN1* and *Phf6* KO+*ICN1* recipients was mainly $CD4^+CD8^+$ cells (supplemental Figure 9B), but we observed that *Phf6* KO+*ICN1* recipients had a higher percentage of CD4 single-positive leukemia cells ($P = .0325$) (Figure 6B). Both WT+*ICN1* and *Phf6* KO+*ICN1* recipients had similar thymus size (supplemental Figure 9C), but recipients' *Phf6* KO+ICN1 cells showed heavier tumor burden in their thymus (supplemental Figure 9D). The *Phf6* KO+*ICN1* mice had larger spleens (Figure 6C) and significantly shorter overall survival ($P < .0001$) (Figure 6D).

Using diluting doses of leukemia cells from these mice for secondary transplantation into recipients 8 to 12 weeks of age, we confirmed that *Phf6* knockout lowered the threshold of *ICN1*-induced transformation: all the WT+*ICN1* mice survived, but almost all *Phf6* KO+*ICN1* mice died, at the lowest dose (1000 cells/mouse) (Figure 6E; supplemental Figure 9E). Through FACS analysis, we confirmed that *Phf6* KO+*ICN1* mice had a higher percentage of LICs ($CD4^-CD8^-CD25^+CD127^+$) in their bone

Figure 4. (continued) n = 21). (C) Aged *Phf6* KO mice had lower $B220^+$ B-cell counts in their peripheral blood compared with wild-type mice ($P = .0345$; wild-type, n = 20; *Phf6* KO, n = 21). (D) Aged *Phf6* KO mice had lower $CD4^+$ T-cell counts in their peripheral blood ($P = .0126$; wild-type, n = 20; *Phf6* KO, n = 21). (E) Aged *Phf6* KO mice had lower $CD8^+$ T-cell counts in their peripheral blood ($P = .0258$; wild-type, n = 20; *Phf6* KO, n = 21). (F) Aged *Phf6* KO mice had larger spleens ($P = .014$; wild-type, n = 7; *Phf6* KO, n = 10). (G) Tissue sections showed increased extramedullary hematopoiesis in the red pulp of spleens from *Phf6* KO mice (inset 20×). (H) Bone marrow sections showed increased megakaryocyte number, decreased cell size, and nuclear lobation of megakaryocytes (indicated by white arrows) in *Phf6* KO mice (inset 1000×; scale bar, 10 μm). (I) Megakaryocytes of aged *Phf6* KO mice had decreased cell size ($P = .0007$; both, n = 3). (J) Aged *Phf6* KO mice had increased megakaryocyte number ($P = .0004$; both, n = 3). (K) Aged *Phf6* KO mice had higher percentages of $CD4^+$ cells (left) and lower percentages of $CD8^+$ cells (right) in the spleens ($P = .0105$ and .0247, respectively; wild-type, n = 5; *Phf6* KO, n = 9). (L) In the fraction of $CD4^+$ splenic T cells, *Phf6* KO mice had higher percentages of naive regulatory T cells (left panel) and lower percentages of effector T cells (right panel) ($P = .018$ and .0205; wild-type, n = 5; *Phf6* KO, n = 9). (M) In the bone marrow, aged *Phf6* KO mice had decreased LT-HSCs ($P = .0424$; wild-type, n = 7; *Phf6* KO, n = 10). $^*P < .05$; $^{***}P < .001$. HPF, high-power field; $TCR\beta^+$, T-cell receptor-β^+.

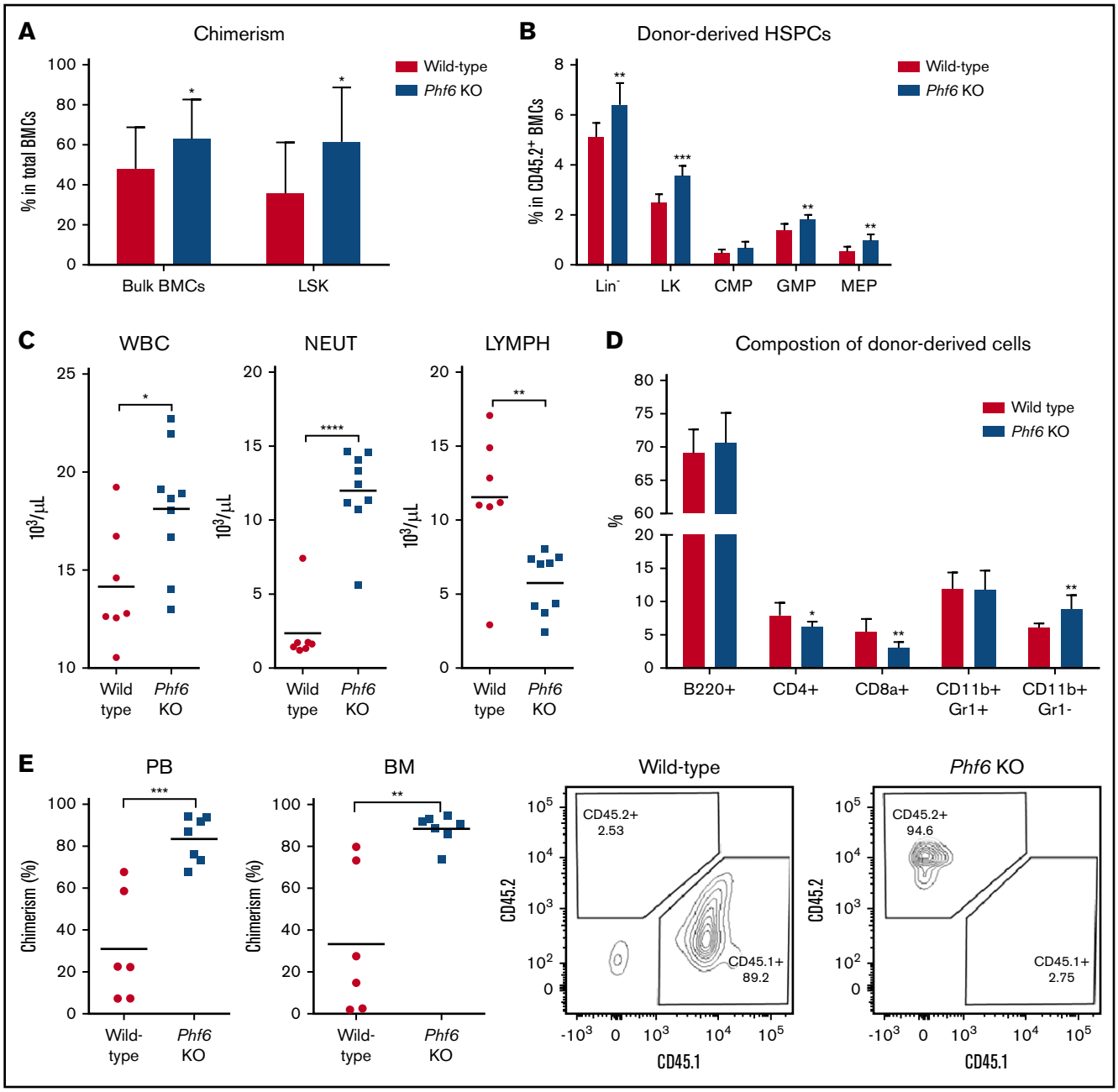

Figure 5. Transplantation assays of *Phf6* knockout (KO) BMCs. (A) Chimerism was higher in the marrow of recipients transplanted with bulk *Phf6* KO BMCs ($P = .0312$; wild-type, n = 7; *Phf6* KO, n = 7). The recipients transplanted with sorted LSK cells from bone marrow of *Phf6* KO mice also had significantly higher chimerism compared with wild-type ($P = .0478$; wild-type, n = 9; *Phf6* KO, n = 8). (B) In a competitive repopulation unit assay, the recipients of *Phf6* KO BMCs had higher percentages of Lin$^-$, LK, GMP, and megakaryocyte-erythroid progenitor (MEP) cells ($P = .0065$, .000169, .0037, and .0032, respectively; wild-type, n = 7; *Phf6* KO, n = 7) among the donor-derived cells. (C) Recipients of *Phf6* KO BMCs had higher WBC and neutrophil (NEUT) counts but lower lymphocyte (LYMPH) counts than those of wild-type BMCs. (D) Within donor-derived blood cells, recipients of *Phf6* KO BMCs had a lower proportion of CD4$^+$ and CD8$^+$ cells but higher CD11b$^+$Gr1$^-$ cells in the blood compared with wild-type BMCs. (E) The chimerism in blood (left panel) and marrow (right panel) of the recipients of *Phf6* KO BMCs was further enhanced in the secondary transplantation. Representative FACS plots of bone marrow are shown. *$P < .05$; **$P < .01$; ***$P < .001$; ****$P < .0001$. CMP, fluorescence-activated cell sorting analysis and cell sorting; PB, peripheral blood.

marrow ($P = .0438$) (Figure 6F).[17] An extreme limiting dilution analysis Web tool also indicated that *Phf6* KO+*ICN1*mice had significantly more LICs; the estimated LIC frequency in WT+*ICN1* and *Phf6* KO+*ICN1* marrow cells were 1 per 8960 and 1 per 576, respectively (Figure 6G).

Transcriptomic analysis of the HSCs from *Phf6* knockout mice and the wild-type littermates

To interrogate the possible molecular mechanisms underlying the distinct phenotypes of *Phf6*-deficient HSCs, we analyzed the

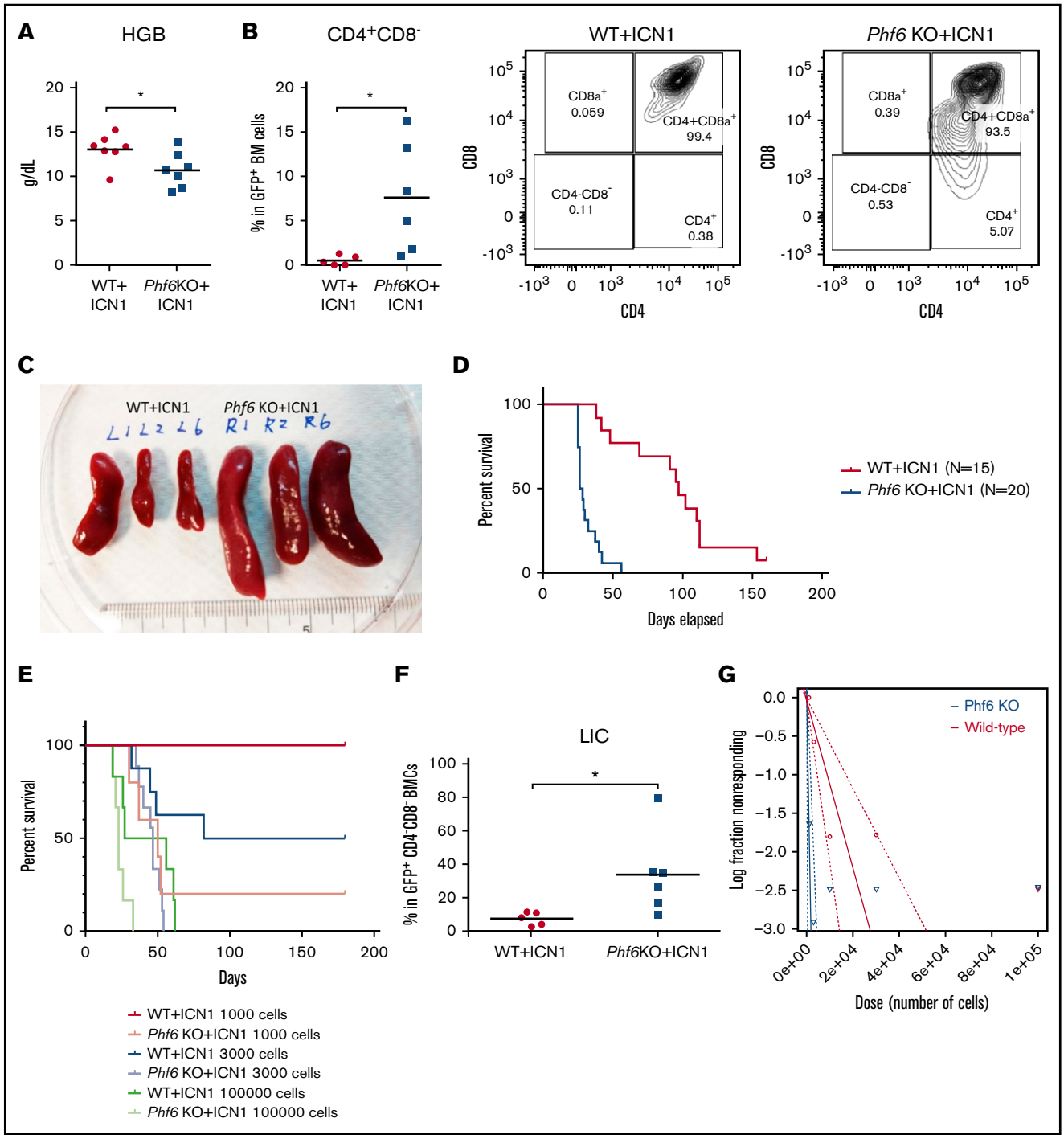

Figure 6. The synergistic effects of *Phf6* deletion on *ICN1* overexpression. (A) Six weeks after transplantation, the recipients of *Phf6* KO+*ICN1* cells had lower hemoglobin (HGB) levels. (B) The recipients of *Phf6* KO+*ICN1* cells had higher percentages of $CD4^+CD8^-$ cells within the *ICN1* overexpressing BMCs ($P = .0325$). Representative FACS plots of bone marrow are shown. (C) The recipients of *Phf6* KO+*ICN1* cells had larger spleens. (D) The recipients of *Phf6* KO+*ICN1* cells had a shorter overall survival ($P < .0001$). (E) The survival disadvantages of *Phf6* KO+*ICN1* mice held true with different cell doses. (F) There were more LICs ($CD4^-CD8^-CD25^+CD127^+$) in *Phf6* KO+*ICN1* mice marrow. (G) *Phf6* KO+*ICN1* mice had more LIC ($P < .0001$) according to limiting dilution assays. *$P < .05$.

transcriptomes of highly restricted, rare subpopulations of HSCs of the mice. We sorted 100 to 200 cells of LT-HSCs, MPP2, and MPP3 from *Phf6* knockout or wild-type animals for transcriptome sequencing. Differentially expressed genes between wild-type and *Phf6* knockout cells were significantly enriched in those associated with cell cycle, leukocyte differentiation, and stem cell differentiation, consistent with our phenotypic analyses (Figure 7A). Gene signatures related to cell cycle–associated functions were enhanced in all 3 subpopulations of *Phf6* knockout HSPCs (Figure 7B); leading edge genes, including *Dna2*, *Gtse1*, *Hras*,

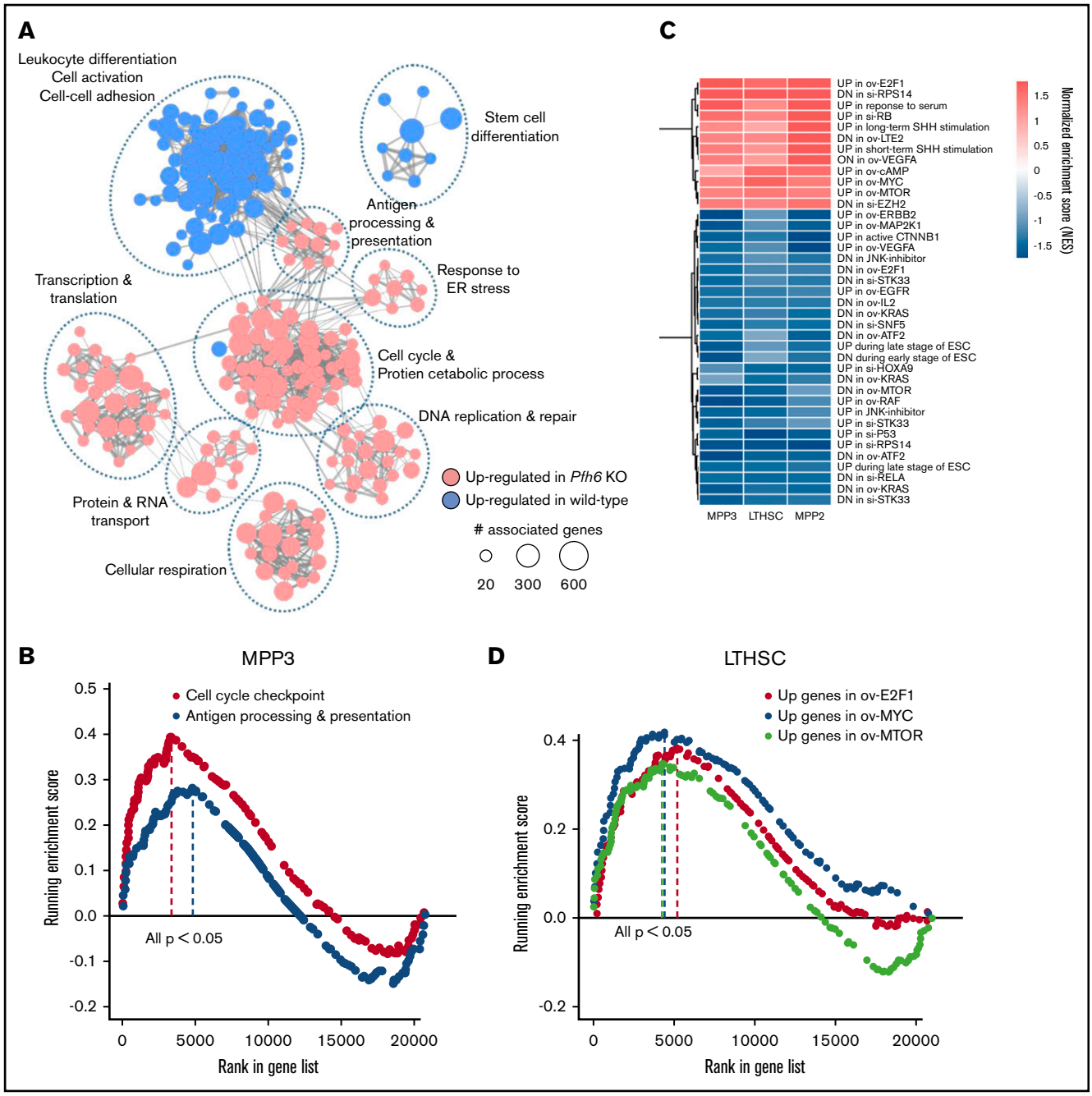

Figure 7. *Phf6* deletion enriched differentiation and cell cycle–associated functions in HSPCs. (A) Enrichment Map showing the significantly perturbed functions in *Phf6*-null compared with wild-type HSPCs nodes are Gene Ontology gene sets, and edges indicate shared genes. (B) GSEA plot for representative gene sets enriched in *Phf6* KO vs wild-type cells. (C) Heatmap representation of oncogenic signatures significantly enriched or depleted ($P < .05$) in *Phf6* KO HSPCs. (D) GSEA plot for representative oncogenic signatures enriched in *Phf6* KO cells vs wild-type cells. E2F1, Myc oncogene (MYC), and MTOR signatures were positively enriched in Phf6 KO LT-HSCs, MPP2, and MPP3. ER, endoplasmic reticulum.

Plk1, and *Zwilch* known to promote cell division, were upregulated in *Phf6* knockout cells[26-30] (supplemental Table 1), consistent with our observation (Figure 3E). The tumor suppressor functions of *Phf6* were corroborated by enrichment of genes implicated in oncogenic functions in *Phf6* knockout HSPCs (Figure 7C; supplemental Table 2); the E2F1, MYC, and mammalian target of rapamycin (mTOR) functions, which were considered to enhance stem cell proliferation,[31-36] were upregulated in all 3 subpopulations of *Phf6* null HSCs (Figure 7D).

Discussion

The goal of the current report was to elucidate the biological functions of PHF6 in hematopoiesis and leukemogenesis by

generation of hematopoietic cell–specific *Phf6* knockout mice. We found that Phf6 regulated self-renewal, reconstitution, and cell cycle of HSCs. Loss of Phf6 resulted in myelodysplasia-like disease in aged mice. In addition, Phf6 functions as a tumor suppressor in ICN-induced T-ALL.

Three studies of *Phf6* knockout mouse models were reported recently.[12-14] All three mouse models were generated by inserting loxP sequences flanking exon 4 and exon 5 of *Phf6*, leaving the zinc knuckle motif in exon 2 and exon 3 intact.[3] Different from these studies, we inserted loxP sequences before exon 2 and after exon 11 of *Phf6*, deleting the entire *Phf6* coding sequence by Cre recombinase. Wendorff et al[12] and Miyagi et al[13] used pan-hematopoietic *vavCre* and inducible *Rosa26-creERT2* to control the sites and timing of *Phf6* knockout; Miyagi et al also used *Mx1-cre* to control the timing of *Phf6* deletion in hematopoietic cells, and McRae et al used *Tie2-cre*, a cre specific to endothelial lineage cells,[37] for hematopoietic- and endothelial-specific deletion of *Phf6*.

The 3 groups[12-14] and our group found that *Phf6*-deleted HSCs had stronger reconstitution capacity compared with wild-type HSCs through transplantation assays. The self-renewal capacity of HSCs was enhanced by *Phf6* knockout in our study and in the studies of Wendorff et al[12] and Miyagi et al[13] but not in the study of McRae et al.[14] Although our study and the study by Wendorff et al showed sensitization to *NOTCH1*-induced transformation by *Phf6* knockout, the study by McRae et al did not report this synergism. In the report of McRae et al, *Phf6*-null mice developed hematopoietic neoplasms after extremely long latency, but we could observe myelodysplastic-like features in mice at 18 months of age. However, Miyagi et al reported that *Phf6* loss did not induce blood malignancies in serial transplantation assays. The reasons for these discrepancies remain unclear but may be related to the different strategies of mouse generation and/or the length of the observation periods.

To clarify the association between differentially expressed genes and the biological functions of HSPCs, we collected LT-HSCs, MPP2, and MPP3 for transcriptome sequencing. Gene ontology and GSEA analyses showed enrichment of a large number of gene sets associated with cell cycle–related functions. Consistent with our findings, McRae et al[14] and Miyagi et al[13] observed that *Phf6* knockout HSPCs are more active in cell cycling. Our transcriptomic analyses on highly restricted subpopulations of HSCs suggest that the phenotype might be at least related to upregulation of genes implicated in cell cycle–associated functions and downregulation of those in differentiation-related pathways (Figure 7A-B). We found that *Dna2*, *Gtse1*, *Hras*, *Plk1*, and *Zwilch* were leading edge genes positively enriched in the cell cycle signature of *Phf6*-null HSPCs. *Gtse1* ensures both chromosome alignment and segregation[29]; *Hras* was an oncogene whose loss was reportedly associated with cell cycle arrest[26]; *Plk1* regulates commitment to mitosis[28]; and *Zwilch* is required for kinetochore functions.[27] These facts are consistent with our finding that *Phf6*-null HSPCs have a more active cell cycle. Specifically, MYC, E2F1, and mTOR pathway signatures in *Phf6*-null HSPCs were upregulated (Figure 7C-D). Previous studies showed that MYC, E2F1, and mTOR augmented self-renewal, proliferation, and metabolism of HSPCs.[32-34,36,38] These genetic alterations may at least partially explain the more active cellular proliferation and division and the oncogenic functions of *Phf6*-null HSPCs.

In conclusion, we have shown the crucial roles of *Phf6* in HSC regulation and the development of leukemia through comprehensive phenotypic and transcriptomic analyses, highlighting the biological functions of Phf6 in physiological and malignant hematopoiesis.

Acknowledgments

The authors thank the technical services provided by Chi-Yuan Yao and the Transgenic Mouse Model Core Facility of the National Core Facility Program for Biotechnology, Ministry of Science and Technology, the Gene Knockout Mouse Core Laboratory of National Taiwan University Center of Genomic Medicine, and the National Center for Genome Medicine. They thank the technical help from the Genomics Core Facility of the Institute of Molecular Biology, Academia Sinica. The authors also acknowledge the service provided by the Flow Cytometric Analyzing and Sorting Core Facilities at National Taiwan University Hospital and First Core Laboratory of National Taiwan University College of Medicine. The authors appreciated the staff of the Eighth Core Laboratory, Department of Medical Research, National Taiwan University Hospital for technical support.

The study was supported by a National Taiwan University Hospital–National Taiwan University joint research grant (UN-106-024), Ministry of Science and Technology of Taiwan (MOST106-2811-B-002-165 and MOST 102-2325-B-002-028), and Ministry of Health and Welfare (MOHW107-TDU-B-211-114009).

Authorship

Contribution: Y.-C.H. wrote the paper, performed the experiments, and analyzed the data; T.-C.C. performed experiments; C.-L.H. performed the bioinformatics analysis; C.-T.Y. interpreted the tissue sections; W.-C.C. and H.-F.T. planned, designed, coordinated the research, and wrote the manuscript; and C.-C.L., H.-A.H., C.-J.K., P.-H.C., and Y.-R.C. provided important materials and help in the study.

Conflict-of-interest disclosure: The authors declare no competing financial interests.

ORCID profiles: Y.-C.H., 0000-0001-5392-2509; C.-L.H., 0000-0002-7447-8045.

Correspondence: Wen-Chien Chou, Department of Laboratory Medicine, National Taiwan University Hospital, No. 7, Chung-Shan S Rd, Taipei City 10002, Taiwan; e-mail: wchou@ntu.edu.tw; or Hwei-Fang Tien, Department of Internal Medicine, National Taiwan University Hospital, No. 7, Chung-Shan S Rd, Taipei City 10002, Taiwan; e-mail: hftien@ntu.edu.tw.

References

1. Landais S, Quantin R, Rassart E. Radiation leukemia virus common integration at the Kis2 locus: simultaneous overexpression of a novel noncoding RNA and of the proximal Phf6 gene. *J Virol*. 2005;79(17):11443-11456.

2. Voss AK, Gamble R, Collin C, et al. Protein and gene expression analysis of Phf6, the gene mutated in the Börjeson-Forssman-Lehmann syndrome of intellectual disability and obesity. *Gene Expr Patterns*. 2007;7(8):858-871.

3. Todd MAM, Picketts DJ. PHF6 interacts with the nucleosome remodeling and deacetylation (NuRD) complex. *J Proteome Res*. 2012;11(8):4326-4337.
4. Wang J, Leung JW, Gong Z, Feng L, Shi X, Chen J. PHF6 regulates cell cycle progression by suppressing ribosomal RNA synthesis. *J Biol Chem*. 2013; 288(5):3174-3183.
5. Zhang C, Mejia LA, Huang J, et al. The X-linked intellectual disability protein PHF6 associates with the PAF1 complex and regulates neuronal migration in the mammalian brain. *Neuron*. 2013;78(6):986-993.
6. Lower KM, Turner G, Kerr BA, et al. Mutations in PHF6 are associated with Börjeson-Forssman-Lehmann syndrome. *Nat Genet*. 2002;32(4):661-665.
7. Chao MM, Todd MA, Kontny U, et al. T-cell acute lymphoblastic leukemia in association with Börjeson-Forssman-Lehmann syndrome due to a mutation in PHF6. *Pediatr Blood Cancer*. 2010;55(4):722-724.
8. Van Vlierberghe P, Palomero T, Khiabanian H, et al. PHF6 mutations in T-cell acute lymphoblastic leukemia. *Nat Genet*. 2010;42(4):338-342.
9. Van Vlierberghe P, Patel J, Abdel-Wahab O, et al. PHF6 mutations in adult acute myeloid leukemia. *Leukemia*. 2011;25(1):130-134.
10. Meacham CE, Lawton LN, Soto-Feliciano YM, et al. A genome-scale in vivo loss-of-function screen identifies Phf6 as a lineage-specific regulator of leukemia cell growth. *Genes Dev*. 2015;29(5):483-488.
11. Soto-Feliciano YM, Bartlebaugh JME, Liu Y, et al. PHF6 regulates phenotypic plasticity through chromatin organization within lineage-specific genes. *Genes Dev*. 2017;31(10):973-989.
12. Wendorff AA, Quinn SA, Rashkovan M, et al. *Phf6* loss enhances HSC self-renewal driving tumor initiation and leukemia stem cell activity in T-ALL. *Cancer Discov*. 2019;9(3):436-451.
13. Miyagi S, Sroczynska P, Kato Y, et al. The chromatin-binding protein Phf6 restricts the self-renewal of hematopoietic stem cells. *Blood*. 2019;133(23): 2495-2506.
14. McRae HM, Garnham AL, Hu Y, et al. PHF6 regulates hematopoietic stem and progenitor cells and its loss synergizes with expression of TLX3 to cause leukemia. *Blood*. 2019;133(16):1729-1741.
15. Georgiades P, Ogilvy S, Duval H, et al. VavCre transgenic mice: a tool for mutagenesis in hematopoietic and endothelial lineages. *Genesis*. 2002;34(4): 251-256.
16. Hu Y, Smyth GK. ELDA: extreme limiting dilution analysis for comparing depleted and enriched populations in stem cell and other assays. *J Immunol Methods*. 2009;347(1-2):70-78.
17. King B, Trimarchi T, Reavie L, et al. The ubiquitin ligase FBXW7 modulates leukemia-initiating cell activity by regulating MYC stability. *Cell*. 2013;153(7): 1552-1566.
18. Jacque E, Schweighoffer E, Tybulewicz VLJ, Ley SC. BAFF activation of the ERK5 MAP kinase pathway regulates B cell survival. *J Exp Med*. 2015; 212(6):883-892.
19. Dobin A, Davis CA, Schlesinger F, et al. STAR: ultrafast universal RNA-seq aligner. *Bioinformatics*. 2013;29(1):15-21.
20. Robinson MD, McCarthy DJ, Smyth GK. edgeR: a bioconductor package for differential expression analysis of digital gene expression data. *Bioinformatics*. 2010;26(1):139-140.
21. Ritchie ME, Phipson B, Wu D, et al. Limma powers differential expression analyses for RNA-sequencing and microarray studies. *Nucleic Acids Res*. 2015;43(7):e47.
22. Yu G, Wang LG, Han Y, He QY. clusterProfiler: an R package for comparing biological themes among gene clusters. *OMICS*. 2012;16(5): 284-287.
23. Merico D, Isserlin R, Stueker O, Emili A, Bader GD. Enrichment Map: a network-based method for gene-set enrichment visualization and interpretation. *PLoS One*. 2010;5(11):e13984.
24. Weng AP, Ferrando AA, Lee W, et al. Activating mutations of NOTCH1 in human T cell acute lymphoblastic leukemia. *Science*. 2004;306(5694): 269-271.
25. Li X, Gounari F, Protopopov A, Khazaie K, von Boehmer H. Oncogenesis of T-ALL and nonmalignant consequences of overexpressing intracellular NOTCH1. *J Exp Med*. 2008;205(12):2851-2861.
26. Bulavin DV, Kovalsky O, Hollander MC, Fornace AJ Jr. Loss of oncogenic H-ras-induced cell cycle arrest and p38 mitogen-activated protein kinase activation by disruption of Gadd45a. *Mol Cell Biol*. 2003;23(11):3859-3871.
27. Williams BC, Li Z, Liu S, et al. Zwilch, a new component of the ZW10/ROD complex required for kinetochore functions. *Mol Biol Cell*. 2003;14(4): 1379-1391.
28. Gheghiani L, Loew D, Lombard B, Mansfeld J, Gavet O. PLK1 activation in late G2 sets up commitment to mitosis. *Cell Reports*. 2017;19(10): 2060-2073.
29. Bendre S, Rondelet A, Hall C, et al. GTSE1 tunes microtubule stability for chromosome alignment and segregation by inhibiting the microtubule depolymerase MCAK. *J Cell Biol*. 2016;215(5):631-647.
30. Hu J, Sun L, Shen F, et al. The intra-S phase checkpoint targets Dna2 to prevent stalled replication forks from reversing. *Cell*. 2012;149(6):1221-1232.
31. Satoh Y, Matsumura I, Tanaka H, et al. Roles for c-Myc in self-renewal of hematopoietic stem cells. *J Biol Chem*. 2004;279(24):24986-24993.
32. Laurenti E, Varnum-Finney B, Wilson A, et al. Hematopoietic stem cell function and survival depend on c-Myc and N-Myc activity. *Cell Stem Cell*. 2008; 3(6):611-624.
33. Wilson A, Murphy MJ, Oskarsson T, et al. c-Myc controls the balance between hematopoietic stem cell self-renewal and differentiation. *Genes Dev*. 2004;18(22):2747-2763.

34. Chen C, Liu Y, Liu R, et al. TSC-mTOR maintains quiescence and function of hematopoietic stem cells by repressing mitochondrial biogenesis and reactive oxygen species. *J Exp Med*. 2008;205(10):2397-2408.

35. Chen C, Liu Y, Liu Y, Zheng P. mTOR regulation and therapeutic rejuvenation of aging hematopoietic stem cells. *Sci Signal*. 2009;2(98):ra75.

36. Xu S, Tao J, Yang L, et al. E2F1 suppresses oxidative metabolism and endothelial differentiation of bone marrow progenitor cells. *Circ Res*. 2018;122(5):701-711.

37. Kisanuki YY, Hammer RE, Miyazaki J, Williams SC, Richardson JA, Yanagisawa M. Tie2-Cre transgenic mice: a new model for endothelial cell-lineage analysis in vivo. *Dev Biol*. 2001;230(2):230-242.

38. Cabezas-Wallscheid N, Buettner F, Sommerkamp P, et al. Vitamin A-retinoic acid signaling regulates hematopoietic stem cell dormancy. *Cell*. 2017;169(5):807-823.e19.